Four-Beam Tiled-Aperture Coherent Beam Combining of High-Power Femtosecond Laser With Two Compressors

Chun Peng, Xunzheng Li, Xiaoyan Liang, and Ruxin Li

***Abstract*—The former reports of coherent beam combining (CBC) in the ultra-intense ultra-short laser field focus on the phase control technology and two-beam CBC. To study the four-beam tiled-aperture CBC in the ultra-intense and ultra-short laser field, we demonstrate four-beam CBC of femtosecond laser pulses based on chirped pulse amplification (CPA) scheme. In this experiment, the four beams were compressed using two grating compressors to simulate the situation in ultra-intense and ultra-short laser CBC systems. To achieve real-time measurement of the phase error between the four beams, we introduced a continuous reference laser and the phases of beams 2, 3, and 4 were locked to beam 1.A combined efficiency of 57% was achieved. Although the coherent combining efficiency is not very high, the possibility of a four-beam CBC based on the CPA scheme was confirmed, especially with different grating compressors which can reduce the limitation of gratings in single beam petawatt lasers. Finally, the remaining difficulties in the implementation of CBC of four beams and the methods to improve its efficiency were analyzed. The use of CBC in ultra-intense and ultrashort laser systems is of considerable significance.**

***Index Terms*—Ultrafast lasers, laser beam combining.**

I. Introduction

HIGH-power laser devices based on chirped pulse amplification (CPA) and optical parametric chirp pulse amplification (OPCPA) techniques can create an ultra-intense laser field. These devices have significantly advanced the development of high-intensity field laser physics, such as astrophysics in the laboratory [1], fast ignition [2], and laser-plasma electron and ion acceleration [3]. Over the last three decades, the peak power of the high-power lasers has increased from several megawatts (MW) to 10 petawatts (PW) [4]–[11]. In the last few years, 100 PW ultra-high and ultra-short laser projects have been proposed by several research centers. A significant restriction for the 100 PW class laser devices is the dimensional limitation of the optical crystals and gratings. To create ultra-high peak power lasers, new techniques have been developed [7], [12]–[16], among these methods, tiled-aperture CBC have been considered to be a most promising way to overcome the limitation of the size of gratings [12]–[14]. The tiled-aperture CBC is suitable for the high-power laser facilities due to its peak intensity enhancement in the focal spots. In a tiled-aperture CBC, several sub-beams propagate through their respective amplifiers and compressors, parallel to the same focusing element. The peak intensity of the CBC focal spots is N^2 of a single sub-beam [17]. Therefore, the final output of the laser is no longer limited by the full size of the crystals and gratings. Tiled-aperture CBC is an effective method for further improving the output capacity of high-power laser devices up to 100 PW.

To improve the feasibility of this technique for ultra-intense ultra-short laser devices, both theoretical and experimental studies have been carried out in high-power laser fields [17]–[22]. However, these studies were mostly based on two sub-beams, with only one article reporting a phasing method of tiled-aperture CBC based on three sub-beams. In 2014, Bagayev reported the experimental realization of tiled-aperture CBC based on OPCPA, verifying the validity of this technique [23] and motivating the potential use of tiled-aperture CBC in ultra-intense ultrashort lasers. In 2014, Marco Kienel [24] reported the realization of two sub-beams that actively controlled the divided pulse CBC in a fiber CPA system. In the same year, Marco Kienel [25] also reported the demonstration of two coherently polarized sub-beams combined with CPA systems, which verified the feasibility of CBC based on CPA structure and bulk amplifiers. In 2019, our group reported the realization of two sub-beams based on the CPA structure and multi-pass Ti:sapphire amplifiers [26]. In 2019, Renqi Liu reported a phasing method for the tiled-aperture CBC of three sub-beams based on a continuous laser, which proposed and verified a practical phasing method for multi-beam tiled-aperture CBC [27]. Multi-beam tiled-aperture CBC is a crucial topic for ultra-intense ultra-short laser field. Nevertheless, tiled-aperture CBC more than two sub-beams based on CPA or OPCPA structures in femtosecond lasers has not

Manuscript received November 24, 2021; accepted November 30, 2021. Date of publication December 3, 2021; date of current version December 28, 2021. This work was supported in part by the National Natural Science Foundation of China under Grants 61775223 and 11974367, in part by the Shanghai Science and Technology Innovation Action Plan Project under Grant 19142202500, in part by the Strategic Priority Research Program of Chinese Academy of Sciences under Grant XDB1603, and in part by the China Postdoctoral Science Foundation under Grant 2020M671240. *(Corresponding author: Xiaoyan Liang.)*

Chun Peng, Xiaoyan Liang, and Ruxin Li are with the State Key Laboratory of High Field Laser Physics, Shanghai Institute of Optics and Fine Mechanics, Chinese Academy of Sciences, Shanghai 201800, China (e-mail: pengchun@siom.ac.cn; liangxy@siom.ac.cn; ruxinli@mail.ac.cn).

Xunzheng Li was with the State Key Laboratory of High Field Laser Physics, Shanghai Institute of Optics and Fine Mechanics, Chinese Academy of Sciences, Shanghai 201800, China. He is now with the Center of Materials Science and Optoelectronics Engineering, University of Chinese Academy of Sciences, Beijing 100049, China (e-mail: lixzh1@shanghaitech.edu.cn).

Digital Object Identifier 10.1109/JPHOT.2021.3132362

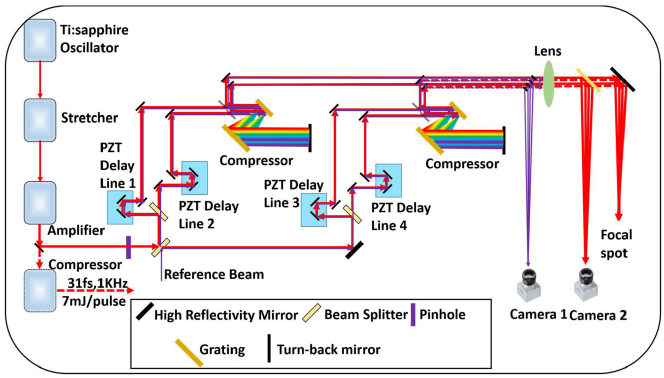

Fig. 1. Experiment setup. Camera 1 is a high-speed camera with a maximum frame rate of 543 fps at the full resolution of 1696 × 1704 pixels. Acquisition speed of camera 1 can be improved to more than 4 K fps by reducing the frame resolution. PZT delay line is based on piezoelectric transition actuator. Each PZT delay line is mounted on a precision mechanical adjustment platform to adjust the optical path difference.

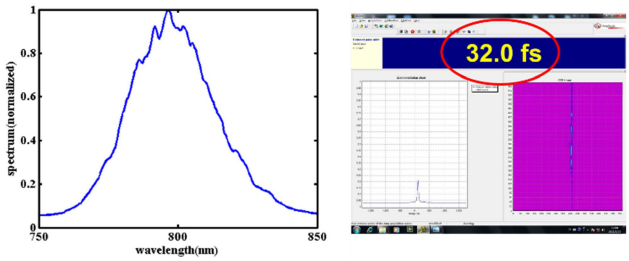

Fig. 2. Spectrum distribution and re-compressed pulse duration of the four sub-beams. Pulse duration is measured by the femtosecond single-shot autocorrelator (Bonsai from Amplitude company), with the right image showing the Bonsai software.

yet been reported. In this study, we performed an experimental demonstration of the four-beam tiled-aperture CBC based on CPA structure.

To our knowledge, this is the first study to implement a tiled-aperture CBC of four sub-beams based on CPA systems in the ultra-intense ultra-short laser field. It was designed to investigate the feasibility of the phasing method in a real four-beam CBC system and experimentally determine the combining efficiency of the system. For simplification, no amplifier was used for the sub-beams. The four beams were arranged in a 2 × 2 square shape in front of the focal lens, which is an effective way to make full use of the mirrors. The four beams were compressed by two grating compressors to study the influence of multiple compressors on CBC, which is of considerable significance in reducing the limitation of the gratings in the ultra-intense ultra-short laser field. The phasing method was based on the near-field interference fringe. To simulate the issues caused by very low repetition for active feedback control of ultra-intense ultra-short laser devices, we introduced a continuous-wave laser as a reference light for phase error measurement.

II. Experimental Setup

The experimental setup is shown in Fig. 1. A commercial CPA femtosecond (fs) laser device consisting of an oscillator, stretcher, amplifier, and compressor was used. The seed pulses were emitted by a Ti:sapphire oscillator centered at 800 nm with a repetition frequency of 80 MHz. The ∼10 fs pulses were stretched to ∼230 ps by the stretcher in the time domain. The repetition was reduced to 1 kHz at the regenerative amplifier, and the energy of the stretched pulses were amplified by the regenerative amplifier to ∼9 mJ/pulse. The full width at half maximum (FWHM) of the spectrum bandwidth after the amplifier was 35 nm. The polarization of the light was vertical, and the diameter was ∼10 mm.

A reflection mirror was incorporated after the amplifier to export the chirped pulses to the four-beam CBC section, with a pinhole cutting the beam diameter to ∼6 mm to fit the size of optical elements. Three 1:1 beam splitters divided the main pulse into four equal sub-beams. Two of the beams passed through PZT delay lines 1 and 2 and were guided into the same compressor. The compressor consisted of two gold-coated gratings (1480 line/mm) and reflective mirrors. The other two beams pass through PZT delay lines 3 and 4 and were guided into another compressor. Finally, the four beams entered the same focal lens in parallel. The spectrum of the four sub-beams is shown in Fig. 2, and the pulse duration was recompressed to ∼32 fs.

The repetition rate of the commercial laser system was 1 kHz. To experimentally study the phasing method of low-repetition CBC between four beams, a reference beam was introduced (purple line in Fig. 1) to measure the piston phase error and feed it back. This is because we can capture the phase error signal at any repetition through the CW laser. A continuous semiconductor laser at 808 nm was used, and the beam was guided into the main system on the opposite side of the first 1:1 splitter of the signal beam. It was divided into four sub-beams and propagated in the same direction as the main beam. This beam was set at a slight angle to spatially separate the reference and main beams before the focal lens. The four sub reference lights are reflected out of the main optical path and guided with a small angle into high-speed camera 1 to create a four-beam interference fringe. Thus, the piston phase errors between the four sub-beams were detected by camera 1 using the near-field interference fringe method [28]. The phase errors between beams 1 and 2, beams 1 and 3, and beams 1 and 4 were derived from the interference fringe by the process computer, and separately fed the phase error signals back to PZT delay lines 2, 3, and 4, respectively. The proportional–integral–derivative (PID) algorithm was used in the processor to enable active control of the phase error.

The compressed femtosecond laser pulses were then focused using a lens with a focal length of 1.6 m. The pattern of the combined laser beams was captured using camera 2 (12-bit). Pictures of the individual and combined beams are displayed in Fig. 4, with (a)–(d) showing the four sub-beams, (e) displaying the incoherent spot pattern with an open loop, and (f) showing the coherent spot pattern with a closed loop. The patterns were gathered at the same attenuation to study the coherent efficiency. It is easy to figure out that, the peak intensity of the coherent

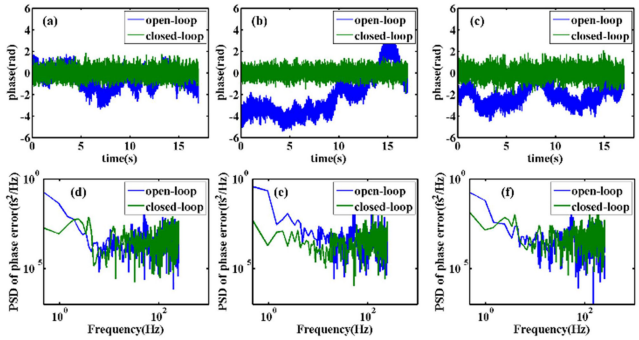

Fig. 3. (a)–(c) Phase differences of beam 1 and beam 2, beam 1 and beam 3, and beam 1 and beam 4, respectively, measured by the near-field interference fringe method for an open-loop (blue line) and a closed-loop (green line); (d)–(f) PSD recorded in the open-loop (blue line) and closed-loop (green line) of beam 1 and beam 2, beam 1 and beam 3, and beam 1 and beam 4, respectively.

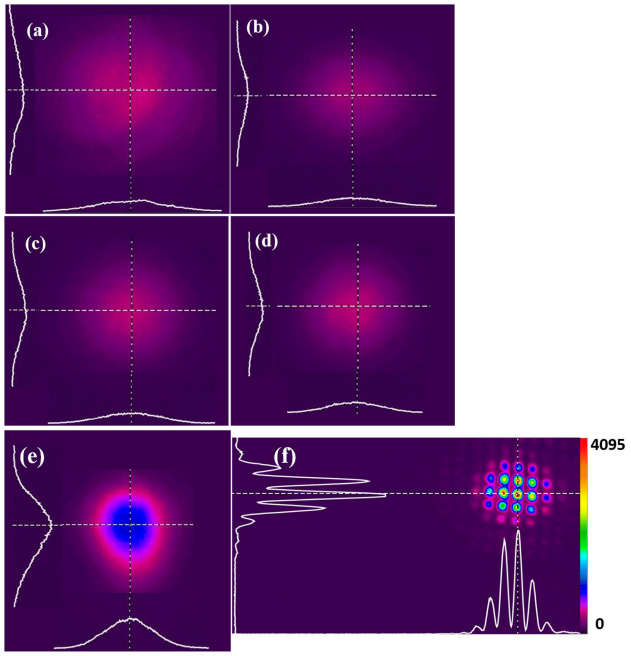

Fig. 4. Beam profiles in the focal plane, with a focal length of 1.6 m. (a)–(d) are the four sub-beams, and (e) and (f) are the four beams combined incoherently and coherently, respectively.

laser beam is several times of the single beams and more than three times of the incoherent one beam.

The CBC theory can be described using Eqs. (1) and (2):

$$I(X,Y,t) = |E(X,Y,t)|^2 = \left| \sum_{m=1}^{M} \sum_{n=1}^{N} E_{m,n}(X,Y,t) \right|^2,$$

$$E(X,Y,t) = \sum_{m=1}^{M} \sum_{n=1}^{N} E_{m,n}(X,Y,t) \tag{1}$$

$$= \sum_{m=1}^{M} \sum_{n=1}^{N} \int_0^{\infty} \int_{-\infty}^{\infty} \int_{-\infty}^{\infty} E_{mn}(x,y,\omega) \times \exp[i\phi_{mn}(x,y,\omega)] \exp[-i\frac{\omega}{cf}(Xx+Yy)] \times \exp(i\omega t) d\omega dx dy, \tag{2}$$

where $E_{m,n}(X,Y,t)$ is the far-field optic field distribution of the (m, n) beam, $E_{mn}(x,y,\omega)$ is the near-field optical field distribution of the (m, n) beam, and $\phi_{mn}(x,y,\omega)$ is the near-field phase of the (m, n) beam.

The CBC efficiency is normally described by the peak intensity recorded by the spot pattern according to the following equation:

$$\eta = \frac{I_\Sigma}{\left(\sqrt{I_1} + \sqrt{I_2} + \sqrt{I_3} + \sqrt{I_4}\right)^2}, \tag{3}$$

where I_Σ is the peak intensity of the far-field spot of the coherently combined pulses, and I_1, I_2, $I_3$and I_4 are those of the single beams.

III. Experiment and Results

The phase errors of the open-loop and closed-loop between beam 1 and beams 2, 3, and 4 were recorded by the processor, as shown in Fig. 3. In this experiment, the phases of beams 2, 3, and 4 were locked to beam 1 through the active control loop in beams 2, 3, and 4. It can be seen from the figure that the phase error is controlled when the active feedback loop is closed. The root-mean-square (RMS) of the controlled phase errors between beam 1 and beams 2, 3, and 4 were 0.47, 0.42, and 0.54 rad, respectively, and the mean values were 0.004, 0.008, and 0.0008 rad, respectively. The power spectral density (PSD) of the phase errors (relative phase fluctuation between the two sub-beams) are shown in Fig. 3(d)–(f). These curves illustrate that the fluctuation of the relative phase is effectively controlled, particularly below 100 Hz.

The maximum intensity of the beam can be obtained from the peak pixel value of the focal spot pattern seen in Fig. 4. The peak intensity of each sub-beam is 480, 380, 480, 460, the incoherently combined one is 1300 and the coherently combined is 4095. The CBC efficiency was 57%, as calculated by Eq. (3). Although the combining efficiency is not as high as that of the previously reported CBC of two beams (∼90%), the results are of great significance for four-beam CBC. In our experiment, the phase error between each two beams is locked to the same level with the previous two-beam CBC [24], and the two-beam CBC efficiency is ∼90% (for example beam 1 and beam 2), corresponding to theoretical four-beam CBC efficiency ∼73%. The decline of the peak intensity of the CBC may caused by the inhomogeneous distribution and alignment error of the focal spots which can be seen from the decline of the incoherently combined intensity. For the reason that the coherently combined peak intensity is still more than three times that of the incoherent one, the experiment is meaningful for the practical four-beam CBC. Moreover, two grating compressors were used in this experiment, which can effectively reduce the required dimensions of the grating. This demonstrates the potential of multi-beam CBC to improve the output of ultra-intense and ultra-short lasers without extremely large gratings.

When locking the phases of beams 2, 3, and 4 to beam 1, the phases of beams 1 and 2 remain relatively stable, as do beams 1 and 3, and beams 1 and 4. However, the absolute phase values of

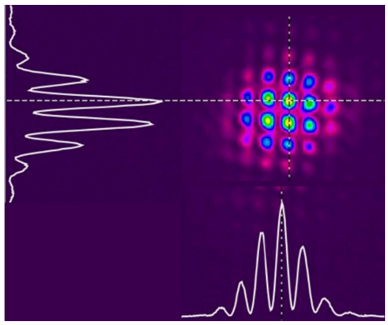

Fig. 5. Beam profiles in the focal plane when the phase lock point is not well matched to the focal spot (the focal length is 1.6 m).

the beams may not remain the same, thus causing a decline in the combining efficiency, as shown in Fig. 5. To obtain the highest combining efficiency, the locking point of beams 2, 3, and 4 should be adjusted by observing the peak density of the focal spot. In our experiment, we adjust the locking point manually according to the peak intensity of the focal spots from Fig 5 to Fig 4, which increasing the combing efficiency from 45% to 57%.

However, when locking the phase of beams 2, 3, and 4 to beam 1, it is difficult to adjust the locking point manually. This is a major factor influencing the low combining efficiency, as it is difficult to determine the right beam to adjust. Our group proposed a method utilizing deep learning of the coherently combined focal spot [29], which could address this problem. In subsequent studies, we will assess this method experimentally.

IV. Conclusion

In this study, we experimentally demonstrated a CBC system of four beams based on the CPA scheme. To achieve real-time measurement of the phase error between the four beams, we introduced a continuous reference laser. The phase errors between beams 2, 3, 4, and 1 were measured and actively controlled, implying that the phases of beams 2, 3, and 4 were locked to beam 1. The combined efficiency of this CBC system of four beams was approximately 57%. The results show that the coherent combined peak density is much higher than that of the incoherent combined focal spot. This experiment verified the possibility of a four-beam CBC based on the CPA scheme, especially with different grating compressors which can reduce the limitation of gratings in single beam petawatt lasers. This is of considerable significance for the potential use of CBC for ultra-intense and ultrashort laser systems.

References

[1] S. Fujioka *et al.*, "X-ray astronomy in the laboratory with a miniature compact object produced by laser-driven implosion," *Nat. Phys.*, vol. 5, 2009, Art. no. 821.

[2] R. Kodama *et al.*, "Fast heating of ultrahigh-density plasma as a step towards laser fusion ignition," *Nature*, vol. 412, 2001, Art. no. 798.

[3] G. A. Mourou, T. Tajima, and S. V. Bulanov, "Optics in the relativistic regime," *Rev. Mod. Phys.*, vol. 78, 2006, Art. no. 309.

[4] K. Yamakawa, M. Aoyama, S. Matsuoka, H. Takuma, C. P. J. Barty, and D. Fittinghoff, "Generation of 16-fs, 10-TW pulses at a 10-Hz repetition rate with efficient ti:Sapphire amplifiers," *Opt. Lett.*, vol. 23, 1998, Art. no. 525.

[5] T. J. Yu, S. K. Lee, J. H. Sung, J. W. Yoon, T. M. Jeong, and J. Lee, "Generation of high-contrast, 30 fs, 1.5 PW laser pulses from chirped-pulse amplification ti:Sapphire laser," *Opt. Exp.*, vol. 20, 2012, Art. no. 10807.

[6] Y. Chu *et al.*, "High-contrast 2.0 petawatt ti: Sapphire laser system," *Opt. Exp.*, vol. 21, 2013, Art. no. 29231.

[7] C. Danson *et al.*, "Petawatt and exawatt class lasers worldwide," *High Power Laser Sci.*, vol. 7, 2019, Art. no. e54.

[8] M. Galletti *et al.*, "Ultra-broadband all-OPCPA petawatt facility fully based on LBO," *High Power Laser Sci.*, vol. 8, 2020, Art. no. e31.

[9] L. Yu *et al.*, "Optimization for high-energy and high-efficiency broadband optical parametric chirped-pulse amplification in LBO near 800 nm," *Opt. Lett.*, vol. 40, 2015, Art. no. 3412.

[10] Z. Gan *et al.*, "200 J high efficiency ti:Sapphire chirped pulse amplifier pumped by temporal dual-pulse," *Opt. Exp.*, vol. 25, 2017, Art. no. 5169.

[11] W. Li *et al.*, "339 J high-energy ti:Sapphire chirped-pulse amplifier for 10 PW laser facility," *Opt. Lett.*, vol. 43, 2018, Art. no. 5681.

[12] K. L. Baker, D. Homoelle, E. Utterback, and S. M. Jones, "Phasing rectangular apertures," *Opt. Exp.*, vol. 17, 2009, Art. no. 19551.

[13] J.-P. Chambaret *et al.*, "Extreme light infrastructure: Architecture and major challenges," in *Proc. SPIE*, 2010, vol. 7721, Art. no. 77211D.

[14] A. V. Bashinov, A. A. Gonoskov, A. V. Kim, G. Mourou, and A. M. Sergeev, "New horizons for extreme light physics with mega-science project XCELS," *Eur. Phys. J. Spec. Top.*, vol. 223, 2014, Art. no. 1105.

[15] S. Kobtsev, "Method of laser pulse amplification," in *Proc. Novel Opt. Syst., Methods, and Appl. XXIV*, San Diego, CA, USA, 2021, vol. 11815, Art. no. 118150S.

[16] V. M. Malkin, G. Shvets, and N. J. Fisch, "Fast compression of laser beams to highly overcritical powers," *Phys. Rev. Lett.*, vol. 82, 1999, Art. no. 4448.

[17] H. Chosrowjan *et al.*, "Interferometric phase shift compensation technique for high-power, tiled-aperture coherent beam combination," *Opt. Lett.*, vol. 38, 2013, Art. no. 1277.

[18] J. Mu *et al.*, "Coherent combination of femtosecond pulses via non-collinear cross-correlation and far-field distribution," *Opt. Lett.*, vol. 41, 2016, Art. no. 234.

[19] Y. Cui *et al.*, "High precision and large range timing jitter measurement and control of ultrashort laser pulses," *IEEE Photon. Technol. Lett.*, vol. 28, no. 20, pp. 2215–2217, Oct. 2016.

[20] C. D. Nabors, "Effects of phase errors on coherent emitter arrays," *Appl. Opt.*, vol. 33, 1994, Art. no. 2284.

[21] Y. C. Yang, H. Luo, X. Wang, F. Q. Li. X. J. Huang, B. Feng, and F. Jing, "Wave optics simulation approach for high-power laser beam combination," *Opt. Commun.*, vol. 284, 2011, Art. no. 3207.

[22] Y. Q. Gao *et al.*, "Phase control requirement of high intensity laser beam combining," *Appl. Opt.*, vol. 51, 2012, Art. no. 2941.

[23] S. Bagayev, V. Leshchenko, V. Trunov, E. Pestryakov, and S. Frolov, "Coherent combining of femtosecond pulses parametrically amplified in BBO crystals," *Opt. Lett.*, vol. 39, 2014, Art. no. 1517.

[24] M. Kienel, A. Klenke, T. Eidam, S. Hädrich, J. Limpert, and A. Tünnermann, "Energy scaling of femtosecond amplifiers using actively controlled divided-pulse amplification," *Opt. Lett.*, vol. 39, 2014, Art. no. 1049.

[25] M. Kienel *et al.*, "Coherent beam combination of Yb:YAG single-crystal rod amplifiers," *Opt. Lett.*, vol. 39, 2014, Art. no. 3278.

[26] C. Peng, X. Liang, R. Liu, W. Li, and R. Li, "Two-beam coherent combining based on Ti:Sapphire chirped-pulse amplification at the repetition of 1 Hz," *Opt. Lett.*, vol. 44, 2019, Art. no. 4379.

[27] R. Liu, C. Peng, W. Wu, X. Liang, and R. Li, "Coherent beam combination of multiple beams based on near-field angle modulation," *Opt. Exp.*, vol. 26, no. 2, 2018, Art. no. 2045.

[28] C. Peng, X. Liang, R. Liu, W. Li, and R. Li, "High-precision active synchronization control of high-power, tiled-aperture coherent beam combining," *Opt. Lett.*, vol. 42, no. 19, 2017, Art. no. 3960.

[29] R. Liu, C. Peng, X. Liang, and R. Li, "Coherent beam combination far-field measuring method based on amplitude modulation and deep learning," *Chin. Opt. Lett.*, vol. 18, 2020, Art. no. 041402.